The locus of recognition memory signals in human cortex depends on the complexity of the memory representations

D. Merika W. Sanders[1,*] and Rosemary A. Cowell[2]

[1]Department of Psychology, Harvard University, Cambridge, MA 02138

[2]Department of Psychological and Brain Sciences, University of Massachusetts Amherst, Amherst, MA 01003

Running title: Recognition memory in visual cortex

*Corresponding author:

D. Merika W. Sanders, merikasanders@fas.harvard.edu

Pages: 45

Figures: 6

Tables: 3

Abstract: 200 words

Introduction: 1012 words

Discussion: 1304 words

Conflict of interest: The authors declare no competing financial interests.

Abstract

According to a "Swiss Army Knife" model of the human brain, cognitive functions such as episodic memory and face perception map onto distinct neural substrates. In contrast, representational accounts propose that the role of each brain region is best explained not by which specialized function it performs, but by the type of information it represents with its neural firing. In a functional MRI study, we examined whether the neural signals supporting recognition memory fall mandatorily within the medial temporal lobes (MTL), traditionally thought the seat of declarative memory, or whether these signals shift within the brain according to the content of the memory. Participants studied objects and scenes that comprised unique conjunctions of pre-defined visual features. Next, we tested participants' recognition memory in a task that required mnemonic discrimination of both simple features and complex conjunctions. Feature memory signals were strongest in early visual regions, declining towards the MTL, while conjunction memory signals followed the opposite pattern. Moreover, feature memory signals correlated with feature memory discrimination performance most strongly in posterior visual regions, whereas conjunction memory signals correlated with conjunction discrimination performance most strongly in the MTL. Thus, recognition memory signals shifted with changes in memory content, supporting representational accounts.

Keywords: modularity; recognition memory; representational accounts; ventral visual pathway; visual perception

The Swiss Army knife analogy of brain function (Cosmides and Tooby 1994) asserts that the human mind contains many functionally distinct cognitive “tools” – e.g., for language acquisition, reinforcement learning, visual perception – each employing different mechanisms that emerged as independent adaptive specializations. This analogy has greatly influenced cognitive neuroscience, encouraging researchers to focus on the separability of cognitive functions and map them to distinct neuroanatomical substrates (e.g., Aggleton and Brown 1999; Kanwisher 2006; Duncan et al. 2019). Applied to memory, the Swiss Army knife analogy manifests as the “Multiple Memory Systems” tradition, under which theories of memory posit multiple separable systems for different modes of learning and storage, underpinned by distinct neural substrates (Sherry and Schacter 1987; Tulving 1987; Tulving and Schacter 1990; Nadel 1992). More recently, some theories derived from this general framework have rejected one-to-one mappings between cognitive functions and focal brain structures, instead mapping mnemonic functions to distributed networks (Ranganath and Ritchey 2012; Rugg and Vilberg 2013; Thakral et al. 2017; Hebscher and Voss 2020). However, an important legacy of the Swiss army knife view is that most research questions still center on a cognitive function, such as episodic memory retrieval, and ask which brain region, distributed network, or neural mechanism supports it. That is, cognition is still carved into subdomains that correspond to functional "tools", and these tools still serve as the cognitive constructs whose (putatively fixed) neural substrates must be identified (Cowell et al. 2019).

A partial departure from this approach has been made by theories that invoke information content to explain the roles of different brain regions in memory (e.g., Davachi 2006; Diana et al. 2007; Shimamura 2011). But many such accounts still explain brain

regions' contributions via a *combination* of function and content, e.g., claiming the hippocampus (HC) underpins recollection (a mnemonic function) of contextual details (a type of content; Davachi et al. 2003; Eichenbaum et al. 2007; Staresina et al. 2011, 2013; Bastin et al. 2019). We and others have suggested that "content" is more than just a label to be used *in combination with* mnemonic functions or processes, such as recollection; instead, it may be the primary principle driving how memory and perception map onto the brain at the systems level (Bussey and Saksida 2002; Graham et al. 2010; Nadel and Peterson 2013; Cowell et al. 2019).

One theory that departs fully from the Multiple Memory Systems tradition is the representational-hierarchical account of perception and memory (Bussey and Saksida 2007; Cowell et al. 2010). This account proposes that the role of each brain region within the ventral visual-medial temporal lobe (MTL) pathway is best explained not by which cognitive function it performs, but by the type of information it represents. Building on well-established evidence for a hierarchy of increasingly complex stimulus representations in visual cortex (Hubel and Wiesel 1965; Felleman and Van Essen 1991; Kobatake and Tanaka 1994; Malach et al. 1995; Kanwisher et al. 1997; Kamitani and Tong 2005; Ostwald et al. 2008; Henriksson et al. 2008; Kriegeskorte et al. 2008; Brouwer and Heeger 2009; Serences, Saproo, et al. 2009; Drucker and Aguirre 2009; Cowell et al. 2017), this account suggests that the representational hierarchy extends beyond visual cortex into the MTL. Thus, the pathway houses a graded continuum of representations, beginning with simple visual features such as oriented lines in V1 and culminating in complex multi-modal conjunctions corresponding to episodes or events in HC. Under this account, any region in the pathway should contribute to any perceptual or mnemonic function – e.g., visual

discrimination, mnemonic encoding, or retrieval from declarative memory (including via familiarity signaling or pattern completion-like recall) – if it contains neural representations that are useful for the task.

One prediction of this account is that the MTL contributes to perception of complex stimuli such as 3-dimensional objects and complex spatial scenes – this contradicts the "Multiple Memory Systems" notion that the MTL specializes in long-term, declarative memory (Squire and Zola-Morgan 1991). Much empirical work now supports this prediction (e.g., Buckley et al. 2001; Lee et al. 2005, 2012; Bartko et al. 2007). Indeed, the multi-faceted functional contributions of the MTL are now known to extend to statistical learning (e.g., Schapiro et al. 2014), decision-making (e.g., Palombo et al. 2015), and future simulation (e.g., Thakral et al. 2020) – notably, almost always for tasks involving complex or associative stimuli.

Thus, a key plank of the evidence for a one-to-one mapping between long-term, declarative memory and the MTL has been eroded: we know that the MTL performs non-mnemonic functions. The complementary plank of evidence for this one-to-one mapping concerns whether long-term, declarative memory can be supported by structures outside of the MTL. The representational-hierarchical account suggests that it can, but this prediction has not been thoroughly tested. Some recent studies suggest support for it: early visual regions underlie recognition memory for orientation (Cooke et al. 2015) and spatial location (Thakral et al. 2013; Karanian and Slotnick 2018); pattern completion-based recollection occurs outside of HC for stimuli that do not contain rapidly-learned associations (Ross et al. 2018; Gardette et al. 2022). But, to our knowledge, no study has examined whether recognition memory signals can be made to shift location within the

brain by systematically manipulating the complexity of the representations that must be recognized.

We tested this prediction with an fMRI study of recognition memory in humans. We constructed visual objects and scenes defined by unique conjunctions of precisely specified features. This allowed us to manipulate the complexity (i.e., simple, feature-level versus complex, conjunction-level) of the representations that need to be retrieved for recognition. During recognition memory retrieval in the scanner, we measured feature-based and conjunction-based mnemonic discrimination performance, along with blood oxygenation level-dependent (BOLD) signatures of feature-based and conjunction-based memory. We predicted, following the representational-hierarchical account, that manipulating the complexity of mnemonic information would shift the location of memory signals within the ventral visual-MTL pathway, from posterior for feature memory to anterior for conjunction memory. Further, we predicted that posterior, feature-based memory signals would be most predictive of feature-based mnemonic discrimination performance, whereas anterior, conjunction-based memory signals would best predict the mnemonic discrimination of conjunctions.

Materials and Methods

Design Overview

We used two visual stimulus sets: novel, 3-D objects and novel, everyday scenes. Each object or scene was composed of the conjunction of three binary features (see Figure 1, Figure 2 and the *Stimuli* section). We tested each participant on two separate days, one for each stimulus set. On each test day, participants first entered the scanner and viewed a stream of object or scene stimuli (fMRI data from this “study phase” are not presented in

this report). Participants exited the scanner for a short break, then returned to the scanner for a recognition memory task involving the object or scene stimuli they had just viewed in the study phase. Test stimuli were either Novel, Recombination, or Familiar. In Novel stimuli, all individual features and conjunctions of features were entirely novel. In Familiar stimuli, both the individual features and the conjunction of those three features had been seen in the study phase, and thus were familiar. In Recombination stimuli, the individual features were familiar from having been studied as parts of other items, but the conjunction of those three features was novel.

We assessed feature memory and conjunction memory – in terms of both behavioral performance and neural signals – by comparing different pairs of memory trial types. To assess behavior, we used *d'*, calculated from hits and false alarms using Signal Detection Theory, to measure mnemonic discriminability. To assess neural memory signals, we used a BOLD signal contrast. We assessed *feature memory* by measuring *d'* and the BOLD contrast for Novel versus Recombination trials. This is because the novelty/familiarity of individual features is the only mnemonic factor discriminating these two trial types (both Novel and Recombination stimuli possess a novel conjunction, but only Novel possess novel features). We assessed *conjunction memory* via *d'* and the BOLD contrast for Recombination versus Familiar trials. Here, the novelty/familiarity of the conjunction of features is the only mnemonic factor discriminating the two trial types (both Recombination and Familiar possess familiar features, but only Recombination possess a novel conjunction). This approach tests feature memory divorced from conjunction memory, and conjunction memory divorced from feature memory, which delivers finer control of the content of mnemonic representations than, for example, earlier work

demonstrating cortical reinstatement in early visual areas during retrieval of visual information (e.g., Thakral et al. 2013).

Participants

Twenty-three participants were recruited from the University of Massachusetts-Amherst community and gave their informed consent. All participants spoke English fluently, had normal or corrected-to-normal vision, no history of neurological illness, and no contraindications for MRI scanning. Participants were compensated $25/hour with an additional performance-based bonus up to $10 per scan session. For statistical tests assessing behavioral performance or neural data, separately (i.e., all tests except those assessing brain-behavior correlations), participants with extreme data point outliers were identified and subsequently excluded across the data (Supplementary Table S1).

Stimuli

Two distinct stimulus sets were created using graphical software: novel 3-D objects and scenes. The novel 3-D objects, called Fribbles, were created using Strata Design 3D CX 7.5 (Williams 1998; Barry et al. 2014). Each Fribble was a unique conjunction of three features (3-D colored components referred to as “tail”, “body”, and “head”) and belonged to a “family” (Figure 1). Within a family, there were two possible variants for each of the tail, body and head features and those variants were unique to that family. Therefore, a family contained eight unique Fribbles corresponding to all possible conjunctions of that family’s binary features. We created four Fribble families.

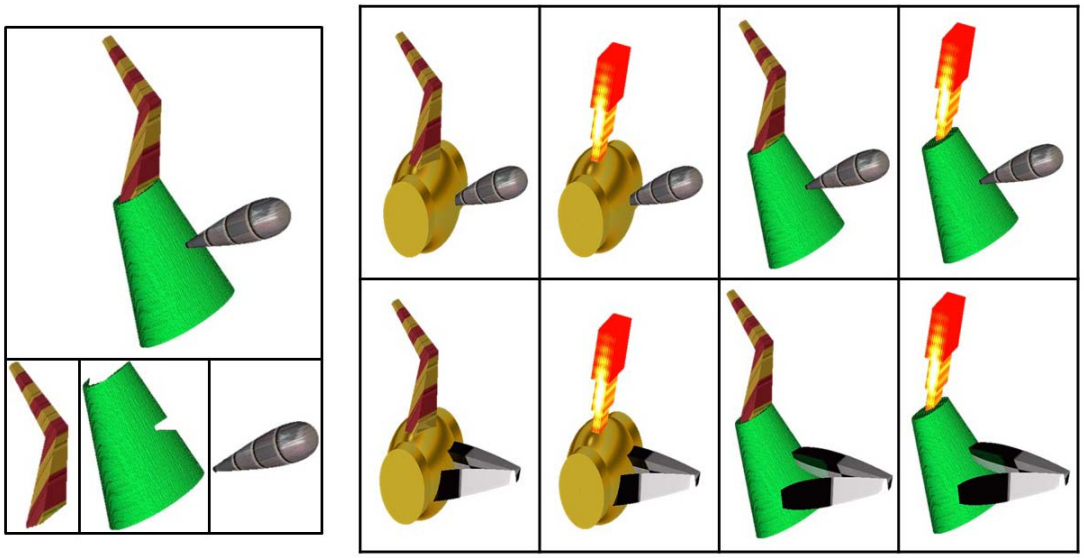

Figure 1. Fribble Stimulus Set Examples. *Left*: A whole, conjunctive Fribble (top) and its tail, body and head features (bottom, left to right); *Right*: A family containing eight unique conjunctive Fribbles, constructed from three binary features (tail, body and head).

Novel scenes were created using Sweet Home 3D, an indoor planning software. Analogous to the Fribbles, each Scene was a unique conjunction of three features ("room shape", "color", and "furniture") and belonged to a "family" (Figure 2). Within a family, there were two possible variants for each feature and those variants were unique to that family. Consequently, each family comprised eight unique Scenes, as for Fribbles. We created four Scene families.

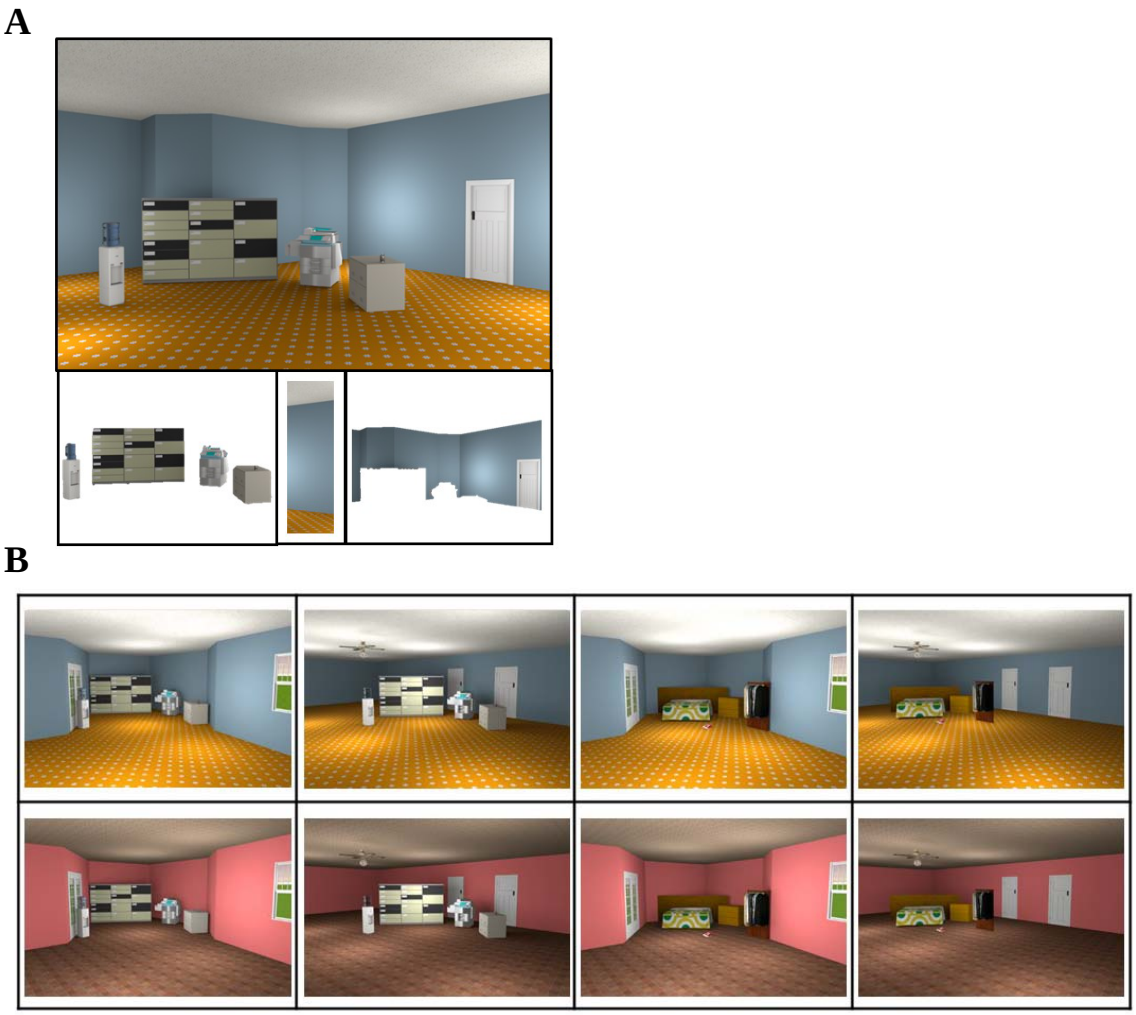

Figure 2. Scene Stimulus Set Examples. *A*: A conjunctive Scene (top) and its features, furniture, color and room shape (bottom, left to right); *B*: A family containing eight unique conjunctive Scenes composed using three binary Scene features.

Task

Tasks were identical for Fribble and Scene stimulus sets. During the study phase, participants completed a 1-back repetition detection task. Some inter-stimulus intervals (ISIs) between study trials contained null trials, during which participants saw a white central fixation cross that dimmed briefly, either once or twice, and participants could press either response key whenever it occurred. No response to 1-back repetitions was

required on the first trial of a run, or on trials immediately following a null. Before entering the scanner, participants practiced this task on a laptop computer.

During the break between study and test, participants received instructions on how to distinguish between the three mnemonic stimulus classes (Familiar, Recombination, and Novel). During test, participants indicated the class of the stimulus on the screen using three button box keys: (1) "Familiar" (studied in the previous session); (2) "Recombination" (made of features studied in the previous session, combined in a new way); or (3) "Novel" (not studied in the previous session in any form). In the test phase, null trials occurred during every ISI.

For both study and test, participants were instructed to respond as accurately as possible while the stimulus was still on the screen, and were informed that a performance-based bonus was available.

Experimental Design

For each of the Fribble and Scene stimulus sets, each participant completed ten study scans, or "runs" (fMRI data not presented here), and six test scans (Figure 3). Stimuli were displayed on a 32" LCD monitor positioned at the head end of the magnet bore, which participants viewed via a mirror on the head coil.

In the study phase, stimulus presentation order was blocked by family within each run (e.g., stimuli from one Familiar family were presented in even-numbered study runs, and from the other Familiar family in odd-numbered runs), but stimuli within a run were presented in random order. Within each study run there were 35 stimulus trials: four repetitions each of eight stimuli from a Familiar family, presented singly on a gray background, plus three items repeated a fifth time to create "immediate repeats" for the 1-

back task. Each stimulus was presented for 2000ms, immediately followed by an ISI of between 2000ms and 8000ms, during which a white central fixation cross appeared on a gray background. The response window for stimulus trials began 500ms after stimulus onset and extended 1000ms into the ISI.

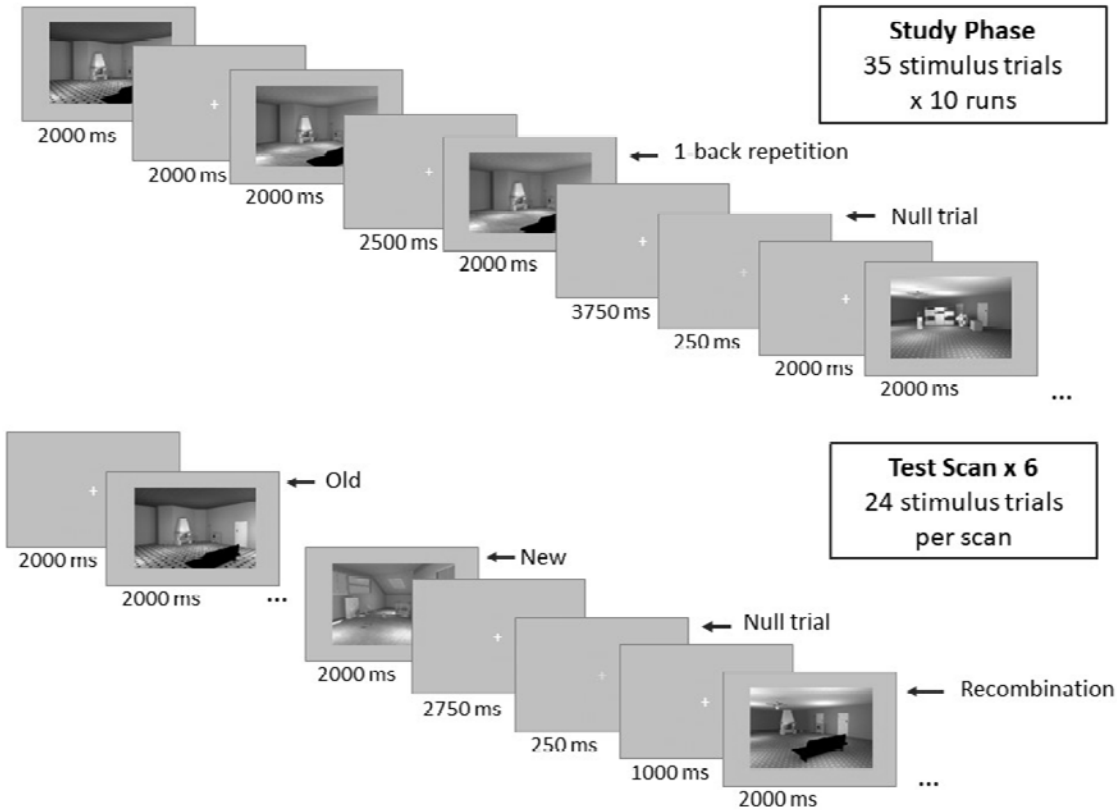

Figure 3. Experimental Design. During the study phase, participants indicated if the current image was identical to the previous image (i.e., 1-back repetition detection task). During the test scan, participants discriminated between Familiar, Novel, and Recombination stimuli. Both the study phase and test scans featured null trials in which participants indicated when a fixation cross dimmed. Scene stimuli are shown here, but the protocol was identical for the Fribble scan sessions, completed on a separate day.

At least 500ms after the end of the response window, for 15 of the 35 ISIs in each study run, a null trial occurred. Null trials occurred only during ISIs of between 3000ms and 8000ms in length. During a null trial, the white cross dimmed to gray for 250ms, either once (for ISIs under 6000ms) or twice (for ISIs 6000 – 8000ms). We randomized the exact

onset of the dimming event(s) within the ISI, with constraints to keep dimming events separate and sufficiently distant from the start or end of the ISI. Null trials measured participants' attention and provided gaps in the sequence with minimal “mind-wandering” (Stark and Squire 2001). After completion of 10 study runs, participants exited the scanner and took a self-paced break before re-entering for the six test runs.

During test runs, 48 Novel, 48 Recombination and 48 Familiar stimulus trials were presented, with 16 unique stimuli from each mnemonic stimulus class shown three times each. Novel and Recombination stimuli were created by combining two features of one family (unstudied for Novel or studied for Recombination) with a third feature of the other unstudied/studied family (Figure 4). Implementing all possible “1 + 2” feature combinations yielded 48 unique stimuli for both Novel and Recombination stimulus classes. However, to match the Familiar stimuli, of which there were only 16 unique exemplars, only 16 out of the 48 possible stimuli were presented for each of Novel and Recombination classes. The subset of 16 stimuli was counterbalanced across participants.

Trial order and spacing of the three stimulus types was determined using the easy-optimize-x MATLAB tool, with the constraints that the three stimulus types appeared equally across the six test runs (i.e., eight of each type per run) and repetition was blocked (i.e., all 48 stimuli were shown once before any stimulus was presented a second time). Each test stimulus appeared for 2500ms, with a randomly assigned ISI between 4000ms and 12000ms. The response window extended 1000ms into the ISI. During every ISI, the null trial commenced only after the response window had elapsed (3500ms after stimulus onset).

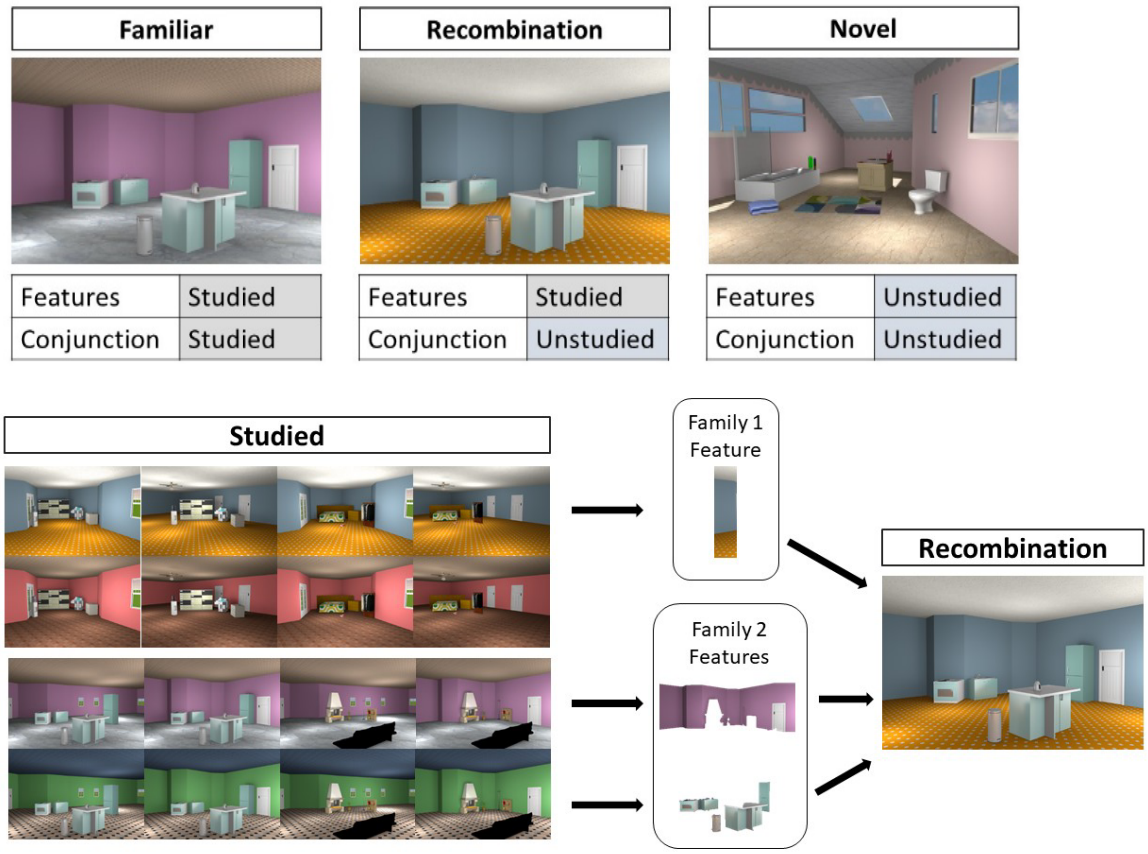

Figure 4. Scene Stimulus Set Recombination Examples. *Top*: the three mnemonic stimulus classes differed according to whether features and the conjunction of features were studied in the study phase; *Bottom*: counterbalanced across participants, two of the Scene families were designated to be studied (i.e., presented in the study phase). In this example, a Recombination stimulus is created by combining the color feature from the first family with the room shape and furniture features from the second family. All potential 1 + 2 feature combinations within a given pair of families yielded 48 Recombination stimuli.

Image Acquisition

Scanning was performed on a Siemens 3T Skyra scanner equipped with a 64-channel head coil at the University of Massachusetts-Amherst's Human Magnetic Resonance Center. Functional images were acquired using a T2-weighted EP2D-BOLD sequence (TR: 1250ms; TE: 33ms; flip angle: 70°; FOV: 210mm; 2.5mm^3 voxels) and forty-two axial slices were acquired during each functional scan. Whole-brain anatomical images were acquired in the middle of the study functional scan session using a T1-weighted

(T1w) MP-RAGE sequence (208 sagittal slices; TR: 2000ms; TE: 2.13ms; flip angle: 9°; 1mm^3 voxels). Functional scans included 20 study runs, 12 test scans and two localizer runs per participant; we used only the data from test runs in the present report.

Data Analyses

fMRI Data Preprocessing

After fMRIPrep's preprocessing pipeline (see Supplementary Materials for details), functional data was high-pass filtered with a 128s cutoff and functional data from test scan sessions underwent smoothing with a 5mm FWHM Gaussian kernel. The data were analyzed with custom MATLAB scripts using SPM 12 software.

Definition of Regions of Interest (ROI)

Despite collecting localizer scans, we ultimately used probabilistic atlases to define ventral visual stream areas (i.e., V1, V2, V3, V3AB, hV4, ventral occipital cortex [VOC], lateral occipital cortex [LOC], temporal cortex [TOC]; Wang et al. 2015) and MTL areas (i.e., parahippocampal cortex [PHC], perirhinal cortex [PRC], HC; Ritchey et al. 2015). In all analyses, data from left and right hemispheres were combined into a single ROI. A subset of representative ROIs were selected for analysis, namely, V1, V2, V3, LOC, PHC, PRC, and HC.

fMRI Memory Score Analysis

To analyze test phase fMRI data, for each stimulus set we constructed a generalized linear model with ten regressors: correct responses to each of Familiar, Recombination and Novel stimulus types; incorrect responses; and six motion nuisance regressors. Each non-motion regressor combined a boxcar model of the stimulus time-series with a canonical

hemodynamic response function. For each participant, the model estimated activation as beta weights (β) for every voxel in each of the four conditions.

Memory signal indices were derived from two contrasts, defined in (1) and (2). To index feature memory, we contrasted beta weights from Novel and Recombination correct trials because the novelty/familiarity of individual features is the mnemonic factor discriminating these trial types (both Novel and Recombination stimuli possess a novel three-feature conjunction, but only Novel stimuli possess novel features). To index conjunction memory, we contrasted the beta weights from Recombination and Familiar correct trials because the novelty/familiarity of the conjunction is the mnemonic factor discriminating these trial types (both Recombination and Familiar stimuli possess familiar features, but only Recombination stimuli possess a novel three-feature conjunction). For feature memory, the beta weights for correct Recombination trials ($\beta_{Recombination}$) were subtracted from the beta weights for correct Novel trials (β_{Novel}). For conjunction memory, the beta weights for correct Familiar trials ($\beta_{Familiar}$) were subtracted from the beta weights for correct Recombination trials ($\beta_{Recombination}$).

For both memory contrasts we obtained a directional Cohen's *d* effect size (mean difference across voxels within an ROI divided by the standard deviation of that difference), to allow comparison of the magnitude of effects across ROIs with different numbers of voxels and different signal-to-noise levels (Rosenthal 1994; Lakens 2013; Erez et al. 2016). Hence:

$$Feature\ Memory\ Score = Cohen's\ d_{\ Feature} = \frac{\bar{x}_{\beta_{Novel} - \beta_{Recombination}}}{sd_{\beta_{Novel} - \beta_{Recombination}}} \quad \#(1)$$

$$Conjunction\ Memory\ Score = Cohen's\ d_{Conjunction} = \frac{\bar{x}_{\beta_{Recombination} - \beta_{Familiar}}}{sd_{\beta_{Recombination} - \beta_{Familiar}}} \quad \#(2)$$

Where $\beta_{Novel} - \beta_{Recombination}$ is a subscript denoting the difference of two vectors: β_{Novel} is a vector of beta weights from all voxels in an ROI on "Novel" trials that were responded to correctly; and $\beta_{Recombination}$ is a vector of beta weights from all voxels in the same ROI on correct "Recombination" trials. Thus, $\bar{x}_{\beta_{Novel} - \beta_{Recombination}}$ is the mean $\beta_{Novel} - \beta_{Recombination}$ difference vector for an ROI, and $sd_{\beta_{Novel} - \beta_{Recombination}}$ is the standard deviation of the $\beta_{Novel} - \beta_{Recombination}$ difference vector across all voxels in the ROI. Analogously, $\beta_{Recombination} - \beta_{Familiar}$ denotes the difference of two vectors: $\beta_{Recombination}$ is a vector from all voxels in an ROI on correct "Recombination" trials; and $\beta_{Familiar}$ is a vector across voxels in the same ROI on correct "Familiar" trials. Thus, $\bar{x}_{\beta_{Recombination} - \beta_{Familiar}}$ is the mean $\beta_{Recombination} - \beta_{Familiar}$ difference vector for an ROI, and $sd_{\beta_{Recombination} - \beta_{Familiar}}$ is the standard deviation of the $\beta_{Recombination} - \beta_{Familiar}$ difference vector.

Correlation of Neural Memory Scores and Behavioral Memory Performance

We assessed recognition memory performance using *d'*. Because there were three trial types (and three possible responses), Familiar, Recombination and Novel, *d'* was calculated for each possible pairwise comparison of trial types, yielding four *d'* scores (Table 1). In each pairwise comparison, trials of the third outstanding trial type were removed from the analysis. Any (erroneous) responses to the two remaining trial types that invoked the outstanding trial type were binned as a hit, miss, false alarm or correct rejection, depending on the comparison.

Two of the four *d'* scores were analogous to the neural feature and conjunction memory scores – Novel vs. Recombination and Recombination vs. Familiar. For these comparisons, we measured the correlation between neural memory scores and recognition memory *d'* scores. For feature memory, we used the Recombination vs. Novel comparison: only Recombination and Novel trials were included, and a "Familiar" response counted as a hit for Recombination stimuli, but a false alarm for Novel stimuli. For conjunction memory, we used the Familiar vs. Recombination comparison: only Familiar and Recombination trials were included, and a "Novel" response counted as a correct rejection for Recombination stimuli, but a miss for Familiar stimuli.

Bayes Factor Analysis

For analyses in which the data allowed for *parametric* statistical tests, we replaced traditional frequentist tests with Bayes Factors (BFs), to assess statistical reliability. Bayesian hypothesis testing offers several advantages over null hypothesis significance testing (NHST), including that BFs quantify the relative evidence of the alternative hypothesis over the null (rather than simply specifying the null and determining whether to reject it); they allow quantitative assessment of the likelihood that the null hypothesis is true (rather than just determining whether it can be rejected); they are not biased against the null hypothesis; and interpretation of a BF is unaffected by the sampling intentions of the experimenter (Wagenmakers et al. 2017). For analyses in which nonparametric tests were required by the structure of the data, we used permutation and shuffling to generate non-parametric null distributions and subsequently assessed whether the statistic produced by the true (unshuffled) data fell in the extreme (>.95) of the generated distribution.

BFs close to 1 indicate that the data are equally likely under both hypotheses, while values much larger than 1 or much smaller than 1 indicate evidence favoring one hypothesis over the other. Categorical guidelines for the interpretation of BFs suggest that values greater than 3 indicate "substantial" evidence for a hypothesis, greater than 10 "strong evidence", greater than 30 "very strong" evidence, and greater than 100 "decisive" evidence (the same guidelines can be applied to the hypothesis in the denominator by making these values fractions; Jeffreys 1961; Raftery 1995).

We used the *BayesFactor* R package (Morey et al. 2015) with default input values for the number of Monte Carlo simulations (10,000) and the scale value for the Cauchy priors ($^1/_2$). The null hypothesis lies in the denominator of the BF, therefore values larger than 1 provide evidence for the alternative hypothesis, e.g., for correlation *t*-tests, BF>1 provides evidence for the alternative hypothesis that there is a significant relationship between the two variables. For ANOVA designs with nested models (i.e., a full model containing all main effects and their interactions, as well as restricted models with fewer effects) all models are compared against the null (i.e., a model with only random subject effects). Because BFs from these nested model comparisons share a common denominator, we can directly compare nested models by taking the ratio of their BFs.

Results

Behavioral Analysis

Performance on the 1-back task during the study phase, measured as the discriminability between same and different trials (*d'*), was good: mean *d'* was 3.21 for Fribbles and 3.26 for Scenes, and there was moderate evidence for the null hypothesis that *d'* values did not differ by stimulus set (BF = 1/.23 = 4.44).

Memory discrimination performance in the test phase (Table 1) was also good, for all comparison types (Familiar vs. Novel (I); Familiar vs. Novel (II); Familiar vs. Recombination; Recombination vs. Novel) for both stimulus sets (Fribbles, Scenes). We explored differences in memory discrimination performance with a BF model comparison akin to a two-way (4x2) ANOVA. The model most favored by the BF analysis included only a main effect of comparison type, indicating that *d'* differed between pairwise comparisons (BF > 150). As expected, *d'* scores were lowest, but still above chance, in the comparison of Familiar and Recombination trials – trials in which all features were familiar, making mnemonic discrimination difficult. Additionally, there was moderate evidence for the null model over the model with only a main effect of stimulus set (BF = 1/.17 = 5.75). Evidence favored additive and interaction models of comparison type and stimulus set over the null model (BF > 150). However, the comparison type-only model fared best: it was favored over the additive and interaction models (in which *d'* differed by stimulus set) with moderate (BF = $2.90 \times 10^{37}/6.17 \times 10^{36} = 4.70$) and strong evidence (BF = $2.90 \times 10^{37}/1.59 \times 10^{36} = 18.30$), respectively. These results together indicate that memory discrimination performance was not influenced by stimulus set.

Table 1: Discriminability of Mnemonic Stimulus Classes for Fribbles and Scenes

Comparison Condition	Fribble	Scene	Trial Types	Hit/Correct Rejection	Miss/False Alarm
Familiar vs. Novel (I)	4.47	4.44	Familiar	"Familiar" & "Recombination"	"Novel"
			Novel	"Novel"	"Familiar" & "Recombination"
Familiar vs. Novel (II)	3.28	3.59	Familiar	"Familiar"	"Novel" & "Recombination"
			Novel	"Novel" & "Recombination"	"Familiar"
Familiar vs. Recombination	2.32	2.47	Familiar	"Familiar"	"Recombination" & "Novel"
a.k.a. Conjunction Memory d'			Recombination	"Recombination" & "Novel"	"Familiar"
Recombination vs. Novel	4.37	4.22	Recombination	"Recombination" & "Familiar"	"Novel"
a.k.a. Feature Memory d'			Novel	"Novel"	"Recombination" & "Familiar"

Note: Behavioral *d'* scores for four pairwise comparisons of trial types. In each comparison, only two of the three trial types were compared, while trials of the third trial type were removed from the analysis. (Trial types included are indicated in the "Trial Types" column). However, because there were three possible *responses* on a given trial, responses that referred to the third outstanding trial type (i.e., the trial type *not* shown in the "Trial Types" column) were binned as a hit, miss, false alarm or correct rejection, depending on the comparison. The treatment of responses referring to the outstanding trial type is indicated in the "Hit/Correct Rejection" or "Miss/False Alarm" columns. For example, in the first comparison, Familiar vs. Novel (I), only Familiar and Novel trials were included, but a participant could still respond "Recombination". If a participant responded "Recombination" to a Familiar trial, it was counted as "Familiar", and contributed to the hit rate; if a participant responded "Recombination" to a Novel trial, it was again counted as "Familiar" and contributed to the false alarm rate. In the second comparison, Familiar vs. Novel (II), the same two trial types were considered, with an alternative treatment of "Recombination" responses: a "Recombination" response to a Familiar trial counted as a miss, and a "Recombination" response to a Novel trial as a correct rejection. We computed only one version of the "Familiar vs. Recombination" and "Recombination vs. Novel" comparisons, because there was only one sensible way to treat the outstanding response type.

fMRI Memory Score Analysis

To interpret the neural memory scores (Cohen's *d*), we computed BFs to compare nested models in an analysis equivalent to a three-way (2x7x2) ANOVA with factors of stimulus set (Fribbles, Scenes), ROI (V1, V2, V3, LOC, PRC, PHC, HC) and memory score type (Feature Memory, Conjunction Memory; Figure 5, though see Supplementary Figure S1 for root mean beta weights by stimulus set). The model most favored by the BF analysis omitted stimulus set and any of its interactions, but included ROI, memory score type and their interaction (BF > 150, compared to the null model). Moderate and very strong evidence, respectively, favored this model over the next two most favored models, which both included some effect of stimulus set (second-best model included stimulus set, ROI, memory score type and [ROI x memory score type]: BF (best against second-best) = $1.77 \times 10^{80} / 4.41 \times 10^{79} = 4.02$; third-best model included stimulus set, ROI, memory score type, [stimulus set x memory score type] and [ROI x memory score type]: BF (best against third-best) = $1.77 \times 10^{80} / 7.57 \times 10^{78} = 23.41$). Further, there was moderate evidence for the null model over the model with only a main effect of stimulus set (BF = 1/.15 = 6.72). In other words, Cohen's *d* was influenced by ROI, memory score type, and the interaction of ROI with memory score type, but not by stimulus set. Consequently, memory scores were collapsed across stimulus sets and submitted to a model comparison analogous to a two-way (7x2) ANOVA, with factors ROI and memory score type (Figure 6; see Supplementary Figure S2 for individual data points).

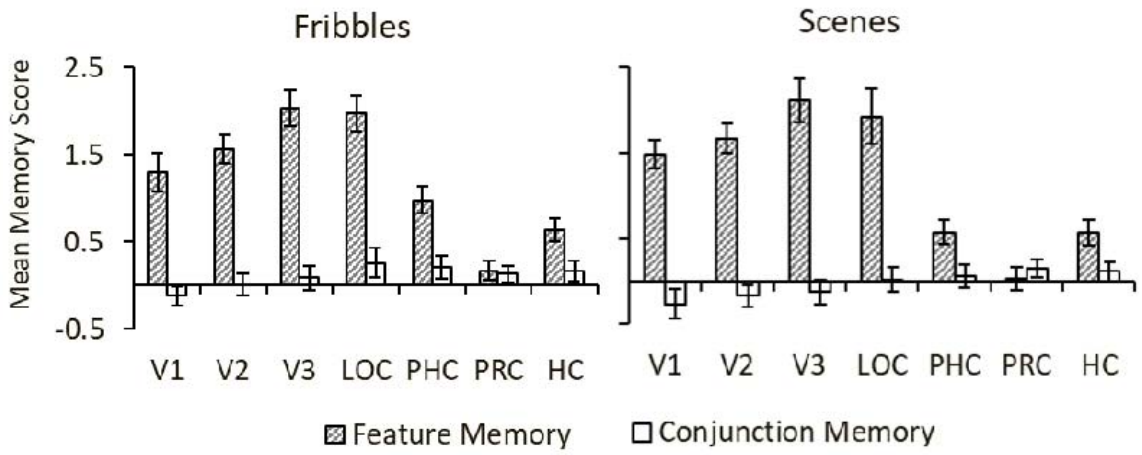

Figure 5. Memory Scores by Stimulus Set Type. Memory scores were derived by calculating the effect size, measured by Cohen's *d*, for the contrast of Novel versus Recombination trials (Feature Memory) and for the contrast of Recombination versus Familiar trials (Conjunction Memory). Error bars are within-subject SEM.

BFs corresponding to the two-way (7x2) ANOVA of memory scores reflected decisive evidence in favor of the interactive model (memory type x ROI) over the null (BF > 150) and over the next two most favored models (additive [memory type + ROI]: BF = 5.83 x 10^{50}/ 2.29 x 10^{32} > 150; memory type only: BF = 5.83 x 10^{50}/ 1.90 x 10^{25} > 150). We explored this interaction by separating the data for feature and conjunction memory and performing two separate model comparisons examining the effect of ROI. We found decisive evidence for a main effect of ROI for feature memory (BF > 150) and substantial evidence for a main effect of ROI for conjunction memory (BF = 8.54). The greatest signal for feature memory occurred in ROIs in early ventral visual stream (V1, V2, V3) and this signal decreased moving anteriorly toward MTL (Figure 6). Additionally, the greatest signal for conjunction memory occurred in MTL (PHC, PRC, HC) and late-stage ventral visual stream (LOC) and decreased moving posteriorly toward early visual areas.

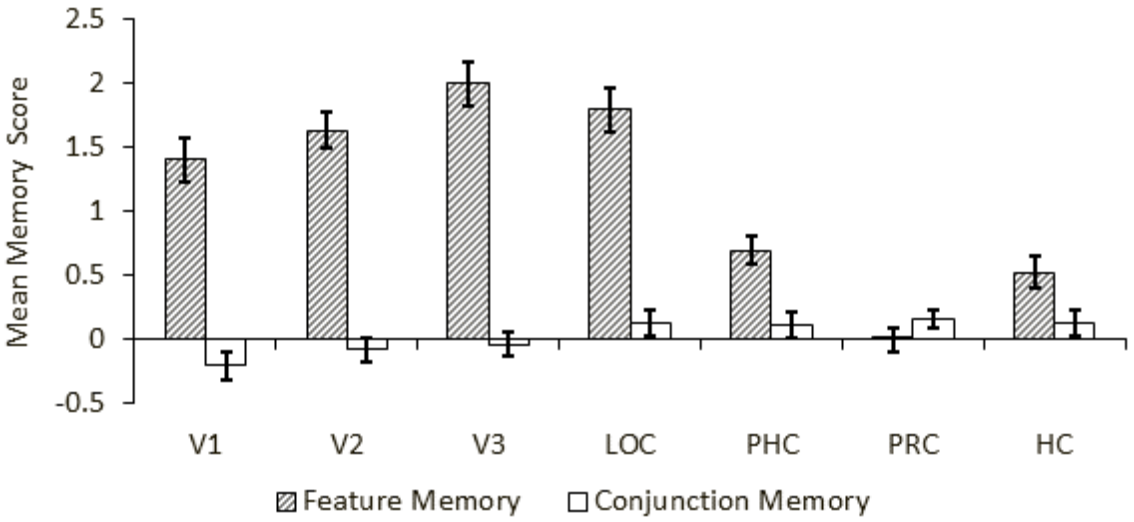

Figure 6. Test Phase Memory Scores. Memory scores, as measured by Cohen's *d*, for the contrast of Novel and Recombination trials (i.e., Feature Memory) and the contrast of Recombination and Familiar trials (i.e., Conjunction Memory). Memory scores were averaged across Fribbles and Scenes for each participant. Striped and solid white bats show group means. Error bars are within-subjects SEM.

Conjunction memory scores clustered near zero, and thus we tested whether any significantly exceeded zero. Of the three individual ROIs with numerically negative conjunction memory scores, there was moderate to strong evidence in favor of the null (i.e., conjunction memory score equaled zero; BF_{V1} = 1/.10 = 10.48; BF_{V2} = 1/.15 = 6.66; BF_{V3} = 1/.19 = 5.27). Of the four individual ROIs with numerically positive conjunction memory scores, there was strong evidence for conjunction memory scores greater than zero in PRC (BF = 13.68) and a lack of substantial evidence for either the alternative or the null in the remainder ROIs (BF_{LOC} = .61; BF_{PHC} = .82; BF_{HC} = 1.18). This suggests a lack of power for detecting conjunction memory signals rather than evidence against conjunction memory.

Correlation of Neural Memory Scores and Behavioral Memory Performance

To assess whether the observed neural signals for feature and conjunction memory are implicated in recognition memory decisions, we correlated neural memory scores

(Cohen's *d*) with recognition memory performance (*d'*) across participants. Specifically, we correlated (1) conjunction memory scores with conjunction memory *d'* (both obtained by comparing Familiar and Recombination trials) and (2) feature memory scores with feature memory *d'* (both obtained by comparing Novel and Recombination trials). We first calculated these correlations separately for each ROI (V1, V2, V3, LOC, PRC, PHC, HC), with neuroimaging and behavioral data averaged across Fribbles and Scenes (Supplementary Figure S3). Pearson correlation coefficients for feature memory were greatest in posterior areas of the ventral visual-MTL pathway, whereas correlation coefficients for conjunction memory were greatest in anterior ventral visual stream and MTL (Table 2). Next, we calculated the same set of correlations separately for each stimulus set (Fribbles and Scenes; Supplementary Figure S4). Pearson correlation coefficients for feature memory were greatest in posterior areas along the ventral visual-MTL pathway for both Fribbles and Scenes. In contrast, correlation coefficients for conjunction memory were greatest in LOC and PRC for Fribbles and in PRC and HC for Scenes (Table 3).

We evaluated the pattern of correlations across ROIs by testing whether the linear trends in correlation coefficients significantly differed between feature and conjunction memory. For each dataset (collapsed over stimulus set; Fribbles alone; Scenes alone), we took the inverse normal transformation of correlations within each ROI, multiplied these by weights describing opposite linear trends for feature memory (i.e., decreasing from early visual areas to MTL) and conjunction memory (i.e., increasing from early visual areas to MTL), and summed the resulting products. For the collapsed and Scenes datasets, we included weights for all seven ROIs (feature memory: [3 2 1 0 -1 -2 -3]; conjunction memory: [-3 -2 -1 0 1 2 3]), but for the Fribbles dataset HC was omitted because we did not

predict, a priori, that object conjunctions would be represented as far anterior as HC, and indeed we had no predictions for the type of code (feature versus conjunction) that HC might contribute for objects (feature memory: [3 2 1 -1 -2 -3]; conjunction memory: [-3 -2 -1 1 2 3]). Next, we generated null distributions for each ROI by shuffling participant Cohen's *d* and *d'* values, computing their correlation, taking the inverse normal transformation of the correlation score, and repeating this 10,000 times. Using the resulting seven ROI null distributions, we performed the difference of linear trends computation described above 10,000 times, to generate a null distribution for the difference of linear trends. If the true trends in correlation across ROIs are similar for feature and conjunction memory, the transformed correlation values multiplied by opposite-trending weights should sum to zero; however, if there are opposite trends in correlation across ROIs, the sum should be greater than zero. When compared to null distributions, the true weighted linear sum was significantly greater than zero for both collapsed and Scenes datasets (collapsed: $p = .01$; Scenes: $p = .007$) and borderline significantly greater than zero for the Fribbles dataset ($p = .06$), indicating that the linear trend of correlation coefficients across ROIs differed for feature and conjunction memory (see Supplemental Figure S5 for permutation distributions).

We next examined which linear trends among the memory type (feature memory, conjunction memory) and dataset (collapsed, Fribbles, Scenes) combinations were significant. For this, we analyzed feature and conjunction memory separately, taking the inverse norm transformed correlation coefficients across ROIs, multiplying by descending weights for feature memory [e.g., 3 2 1 0 -1 -2 -3], or ascending weights for conjunction memory [e.g., -3 -2 -1 0 1 2 3], and summing the product. If there is a linear trend of

correlation coefficients in the direction specified by the weights, the true weighted linear sum should be significantly greater than zero. Compared to null distributions, there was a significant linear trend in the ascending direction for conjunction memory for the collapsed and Scenes datasets (collapsed: p = .02; Scenes: p = .03), and a significant linear trend in the descending direction for feature memory for Scenes (p = .0498). There was no significant linear trend for either feature (p = .10) or conjunction memory (p = .17) for the Fribbles dataset or for feature memory for the collapsed dataset (p = .12; see Supplemental Figure S6 for permutation distributions).

In a final assessment of the relationship between neural memory scores and behavioral memory performance, we calculated BFs to assess the evidence for a correlation in each ROI for each memory type, for all three datasets. As seen in Table 2, for correlations derived from Fribble and Scene datasets combined, the largest BFs for the correlation between feature memory discrimination and neural feature memory scores were found in posterior, visual brain regions. Evidence for a correlation was substantial in regions V1, V2, V3 and LOC, whereas evidence was only anecdotal in all three MTL regions (PHC, PRC, HC). In contrast, the greatest evidence for a correlation between conjunction memory discrimination and neural conjunction memory scores was found in more anterior regions: evidence was anecdotal or modest in V1 through V3, but became very strong in LOC, PHC, PRC, and decisive in HC.

Table 2: Bayes Factors for Correlations between Memory Scores and *d'* for data averaged over Fribbles and Scenes

Memory Type	ROI	BF
Feature Memory Score	V1	4.25
vs.	V2	7.38
Feature memory *d'*	V3	9.61
	LOC	7.78
	PHC	1.31
	PRC	1.20
	HC	1.25
Conjunction Memory Score	V1	1.87
vs.	V2	2.99
Conjunction Memory *d'*	V3	4.03
	LOC	32.60
	PHC	47.78
	PRC	32.63
	HC	107.13

Note: Bayes Factors (BFs) are colored according to which hypothesis is supported by the evidence (green for the alternative hypothesis and red for the null hypothesis) and the strength of support (from palest for anecdotal to darkest for decisive). No color indicates support for neither hypothesis.

Although neither the neural memory scores nor recognition memory performance was affected by stimulus set (Fribbles versus Scenes), it may still be the case that the correlations between neural memory scores and recognition *d'* scores differ between stimulus sets. Table 3 shows the correlations between neural and behavioral memory scores for Fribbles and Scenes, separately. Considering first feature memory, for Fribbles, the strongest evidence for a brain-behavior correlation is found in posterior, visual ROIs, especially V3. Similarly, for Scenes, the largest BF for a feature memory correlation is found in posterior regions, also highest in V3. For both Fribbles and Scenes, there is anecdotal evidence in favor of the null hypothesis, i.e., no correlation, in MTL regions.

Table 3: Bayes Factors for Correlations between Memory Scores and *d'* by Stimulus Set Type

Stimulus Set	**Memory Score**	**ROI**	**BF**
Fribbles	Feature Memory Score	V1	10.60
	vs.	V2	13.34
	Feature memory *d'*	V3	26.60
		LOC	14.74
		PHC	2.77
		PRC	1/0.94 = 1.06
		HC	1/0.34 = 2.94
	Conjunction Memory Score	V1	1.19
	vs.	V2	3.97
	Conjunction Memory *d'*	V3	2.84
		LOC	13.36
		PHC	4.19
		PRC	9.73
		HC	3.83
Scenes	Feature Memory Score	V1	3.52
	vs.	V2	9.77
	Feature memory *d'*	V3	11.07
		LOC	7.29
		PHC	1.06
		PRC	1/0.63 = 1.59
		HC	1/0.69 = 1.45
	Conjunction Memory Score	V1	1.84
	vs.	V2	1.21
	Conjunction Memory *d'*	V3	1.71
		LOC	3.86
		PHC	8.89
		PRC	14.03
		HC	49.42

Note: Bayes Factors (BFs) are colored according to which hypothesis is supported by the evidence (green for the alternative hypothesis and red for the null hypothesis) and the strength of support (palest for anecdotal and darkest for decisive). No color indicates support for neither hypothesis.

Considering next conjunction memory, Fribble and Scene stimuli diverge. Interestingly, the evidence for a brain-behavior correlation in conjunction memory for Fribbles is "strong" only in LOC, an intermediate visual region known for processing objects holistically (e.g., Malach et al. 1995; Grill-Spector et al. 1998), but is approaching "strong" (9.73) in PRC, another region heavily implicated in whole-object processing (e.g., Buckley et al. 2001; Barense et al. 2007). This contrasts with the profile of evidence for a brain-behavior correlation in conjunction memory for Scenes: evidence is absent to anecdotal in posterior regions but increases along the pathway until it reaches "very strong" in HC, suggesting that the conjunction memory signals in HC are most likely to be driving mnemonic discrimination of scene conjunctions.

Discussion

We tested the hypothesis that the neural signals supporting recognition memory shift within the brain according to the complexity of information that participants are asked to recognize. This hypothesis stems from representational accounts, in which the neuroanatomical organization of perception and memory is governed by the type of information each brain region represents, rather than – as under a "multiple memory systems" view – by the type of perceptual or mnemonic function each brain region performs. In this neuroimaging study, we used a recognition memory task that assessed mnemonic discrimination at two levels, one level requiring simpler stimulus representations and the other more complex representations. We tested participants' memory for visual stimuli constructed from conjunctions of pre-defined, binary features. We assayed simple memory by contrasting stimuli that were discriminable only on the basis of the familiarity of their features, and we measured more complex memory by

contrasting stimuli that were discriminable only on the basis of the familiarity of their conjunctions.

We report three main findings. First, the strongest neural signals for long-term (i.e., longer than 30 sec) mnemonic discrimination of visual features lie outside of MTL, in visual cortex. Second, the locus of neural recognition memory signals shifted with the complexity of the stimulus representations required for the mnemonic discrimination: simpler memory signals lay posterior to more complex memory signals within the ventral visual-MTL pathway. Third, these memory signals predicted participants' memory performance, and the strongest brain-behavior correlations for feature-based memory emerged in posterior, visual regions, whereas the strongest correlations for conjunction-based memory emerged in anterior, MTL regions. Linear trend analyses of these brain-behavior correlations revealed trends of opposite direction for features versus conjunctions.

Taken together, the locations of the neural signals for memory, and the correlations of those signals with mnemonic performance, indicate that the ventral visual-MTL pathway supports recognition memory behavior exactly as the Representational-Hierarchical account predicts it should. Moreover, just as predicted by representational accounts, the cortical sites found to be driving feature-based versus conjunction-based memory are the same sites previously found to support feature-based versus conjunction-based visual perception. We highlight here several findings that illustrate this claim.

First, we observed in all three datasets (Fribbles, Scenes, and collapsed) that the correlations between feature-based memory signals and feature-based mnemonic discrimination were strongest in early visual regions (V1 to LOC), and anecdotal or absent in MTL regions, which accords with findings from perceptual studies that feature-based

representations reside in early visual regions (e.g., Hubel and Wiesel 1965; Kobatake and Tanaka 1994; Mazer et al. 2002; Kamitani and Tong 2005; Henriksson et al. 2008; Brouwer and Heeger 2009; Serences, Saproo, et al. 2009). Second, for Fribbles – which are novel, visual objects without semantic meaning, but defined by their unique conjunction – we found the greatest evidence for a brain-behavior correlation for conjunction memory in LOC (BF=13.36) and PRC (BF=9.73). This is important, because LOC and PRC are the two regions among those we tested that are most clearly implicated in holistic visual object-processing as measured with perceptual tasks (e.g., Malach et al. 1995; Grill-Spector et al. 1998; Barense et al. 2007). Third, the more general finding that, for Fribbles, conjunction memory signals were most strongly correlated with conjunction memory performance in anterior sites also accords with previous findings that complex conjunctive representations are found in anterior sites during perceptual tasks (e.g., Desimone et al. 1984; Kobatake and Tanaka 1994; Malach et al. 1995; Kanwisher et al. 1997; Kriegeskorte et al. 2008; Ostwald et al. 2008; Drucker and Aguirre 2009; Cowell et al. 2017). Fourth, for Scenes, evidence for a conjunction memory correlation was again negligible in visual cortex and steadily increased with anterior progression, reaching a maximum not in LOC or PRC, this time, but in HC. This pattern aligns strikingly with data from perceptual processing of scenes, particularly when the demands of the perceptual task require conjunctive representations (Lee et al. 2005, 2006, 2007, 2008). In sum, the cortical sites driving feature- or conjunction- based discrimination in this memory task were the same as those previously found to underpin feature- or conjunction-based processing in perceptual tasks.

To our knowledge, this is the first report of a within-study manipulation of the level of complexity of representations required for long-term mnemonic discrimination. That is,

using the same stimuli and a single task – stimuli comprising binary features combined into conjunctions, along with discrimination between Old, Recombined and Novel memory statuses – we teased apart feature- and conjunction-based memory in terms of both neural signals and behavioral performance. This allowed direct comparison of the two types of memory content, demonstrating that manipulating the level of complexity leads to shifts in the locus of long-term memory signals. Furthermore, the presence of significant brain-behavior correlations for both feature- and conjunction-based memory, in locations well predicted by representational accounts, suggests that these BOLD signatures of memory are not epiphenomenal, but rather reflect the brain signals that drive responses in a long-term recognition memory task.

Many recent empirical studies have demonstrated a critical role for visual cortical representations in visual short-term memory (Harrison and Tong 2009; Serences, Ester, et al. 2009; Christophel et al. 2012, 2017; Jerde et al. 2012; Riggall and Postle 2012; Sprague et al. 2014). But the length of the retention delay in those studies was on the order of seconds, whereas in the current paradigm, the delay between study and recognition test was a minimum of twenty minutes. This suggests that visual cortex is involved in memory not just over brief periods in which active maintenance is required, but for longer periods in which synaptic changes are likely to underlie the observed behavioral changes (Clarke et al. 2010; Cooke and Bear 2010, 2015; Banks et al. 2014).

Another literature that has shown a role for sensory cortices in long-term memory retrieval has couched that role as “cortical reinstatement”, with the reinstatement typically said to be mediated or triggered via the HC (Le Bihan et al. 1993; Eichenbaum 2000; Johnson and Rugg 2007; Bosch et al. 2014; Danker et al. 2017). However, the present

results do not support a hippocampally-triggered reinstatement account. Specifically, we found that memory signals within MTL regions do not robustly predict behavior when the mnemonic discrimination is feature-based, even though signals from these same regions are strongly correlated with behavior for conjunction-based discriminations. That is, the involvement of MTL memory signals appears to come and go with manipulations in the content of the memory, just as was found in recent neuroimaging studies of visual recall (Ross et al. 2018; Gardette et al. 2022). This pattern does not fit with the claim that hippocampal engagement is mandatory for reinstatement. Instead, taken together with the finding that, at least for Scenes, feature-memory is better predicted by visual cortex signals than by MTL signals, the pattern suggests that the neural basis of long-term, declarative recognition memory lies distributed along the ventral visual-MTL pathway according to the content of the memory.

Thus, returning to the Swiss Army knife analogy, the present findings contradict a key plank in the argument for a one-to-one mapping between distinct memory systems and distinct neural substrates: the neural substrates of long-term, declarative memory appear to lie outside of the MTL when the to-be-remembered content is sufficiently simple and purely visual. This finding concurs with other recent studies from labs examining long-term visual memory for simple, visual stimuli (López-Aranda et al. 2009; Thakral et al. 2013; Gavornik and Bear 2014; Cooke et al. 2015; Karanian and Slotnick 2018; Ross et al. 2018). Further, we have demonstrated that recognition memory signals can be made to shift location within the brain by systematically manipulating the complexity of the representations needed for recognition. This supports a representational account of cognition, in which regions of the ventral visual-MTL pathway do not specialize in

circumscribed cognitive functions but contribute flexibly to cognition whenever their representations are important for solving the task.

Acknowledgments

This work was supported by the National Science Foundation (award #1554871 to RAC).

We thank Dave Huber and Jeff Starns for helpful discussions.

References

Aggleton JP, Brown MW. 1999. Episodic memory, amnesia, and the hippocampal-anterior thalamic axis. Behav Brain Sci. 22:425–489.

Banks PJ, Warburton EC, Brown MW, Bashir ZI. 2014. Mechanisms of synaptic plasticity and recognition memory in the perirhinal cortex. 1st ed, Progress in Molecular Biology and Translational Science. Elsevier Inc.

Barense MD, Gaffan D, Graham KS. 2007. The human medial temporal lobe processes online representations of complex objects. Neuropsychologia. 45:2963–2974.

Barry TJ, Griffith JW, De Rossi S, Hermans D. 2014. Meet the fribbles: Novel stimuli for use within behavioural research. Front Psychol. 5:1–8.

Bartko SJ, Winters BD, Cowell RA, Saksida LM, Bussey TJ. 2007. Perceptual functions of perirhinal cortex in rats: zero-delay object recognition and simultaneous oddity discriminations. J Neurosci. 27:2548–2559.

Bastin C, Besson G, Simon J, Delhaye E, Geurten M, Willems S, Salmon E. 2019. An integrative memory model of recollection and familiarity to understand memory deficits. Behav Brain Sci. 42:e281.

Bosch SE, Jehee JFM, Fernandez G, Doeller CF. 2014. Reinstatement of Associative Memories in Early Visual Cortex Is Signaled by the Hippocampus. J Neurosci. 34.

Brouwer GJ, Heeger DJ. 2009. Decoding and reconstructing color from responses in human visual cortex. J Neurosci. 29:13992–14003.

Buckley MJ, Booth MC, Rolls ET, Gaffan D. 2001. Selective perceptual impairments after perirhinal cortex ablation. J Neurosci. 21:9824–9836.

Bussey TJ, Saksida LM. 2002. The organization of visual object representations: A

connectionist model of effects of lesions in perirhinal cortex. Eur J Neurosci. 15:355–364.

Bussey TJ, Saksida LM. 2007. Memory, Perception, and the Ventral Visual-Perirhinal-Hippocampal Stream: Thinking Outside of the Boxes. Hippocampus. 17:898–908.

Christophel TB, Hebart MN, Haynes JD. 2012. Decoding the Contents of Visual Short-Term Memory from Human Visual and Parietal Cortex. J Neurosci. 32:12983.

Christophel TB, Klink PC, Spitzer B, Roelfsema PR, Haynes JD. 2017. The Distributed Nature of Working Memory. Trends Cogn Sci. 21:111–124.

Clarke JR, Cammarota M, Gruart A, Izquierdo I, Delgado-García JM. 2010. Plastic modifications induced by object recognition memory processing. Proc Natl Acad Sci U S A. 107:2652–2657.

Cooke SF, Bear MF. 2010. Visual Experience Induces Long-Term Potentiation in the Primary Visual Cortex. J Neurosci. 30:16304–16313.

Cooke SF, Bear MF. 2015. Visual recognition memory: A view from V1. Curr Opin Neurobiol. 35:57–65.

Cooke SF, Komorowski RW, Kaplan ES, Gavornik JP, Bear MF. 2015. Visual recognition memory, manifest as long-term habituation, requires synaptic plasticity in V1. Nat Ne. 18:262–271.

Cosmides L, Tooby J. 1994. Origins of domain specificity: The evolution of functional organization. In: Hirschfeld L,, Gelman S, editors. Mapping the Mind: Domain-specificity in cognition and culture. New York: Cambridge University Press.

Cowell RA, Barense MD, Sadil PS. 2019. A Roadmap for Understanding Memory: Decomposing Cognitive Processes into Operations and Representations. eNeuro. 6.

Cowell RA, Bussey TJ, Saksida LM. 2010. Functional dissociations within the ventral object processing pathway: cognitive modules or a hierarchical continuum? J Cogn Neurosci. 22:2460–2479.

Cowell RA, Leger K, Serences JT. 2017. Feature-coding transitions to conjunction-coding with progression through human visual cortex. J Neurophysiol. jn.00503.2017.

Danker JF, Tompary A, Davachi L. 2017. Trial-by-Trial Hippocampal Encoding Activation Predicts the Fidelity of Cortical Reinstatement during Subsequent Retrieval. Cereb Cortex. 27:3515–3524.

Davachi L. 2006. Item, context and relational episodic encoding in humans. Curr Opin Neurobiol. 16:693–700.

Davachi L, Mitchell JP, Wagner AD. 2003. Multiple routes to memory: Distinct medial temporal lobe processes build item and source memories. Proc Natl Acad Sci. 100:2157–2162.

Desimone R, Albright TD, Gross CG, Bruce C. 1984. Stimulus-selective properties of inferior temporal neurons in the macaque. J Neurosci. 4:2051–2062.

Diana RA, Yonelinas AP, Ranganath C. 2007. Imaging recollection and familiarity in the medial temporal lobe: a three-component model. Trends Cogn Sci. 11:379–386.

Drucker DM, Aguirre GK. 2009. Different spatial scales of shape similarity representation in lateral and ventral LOC. Cereb Cortex. 19:2269–2280.

Duncan K, Semmler A, Shohamy D. 2019. Modulating the Use of Multiple Memory Systems in Value-based Decisions with Contextual Novelty. J Cogn Neurosci. 31:1455–1467.

Eichenbaum H. 2000. A cortical–hippocampal system for declarative memory. Nat Rev Neurosci 2000 11. 1:41–50.

Eichenbaum H, Yonelinas AP, Ranganath C. 2007. The medial temporal lobe and recognition memory. Annu Rev Neurosci. 30:123–152.

Erez J, Cusack R, Kendall W, Barense MD. 2016. Conjunctive Coding of Complex Object Features. Cereb Cortex. 26:2271–2282.

Felleman DJ, Van Essen DC. 1991. Distributed hierarchical processing in the primate cerebral cortex. Cereb Cortex. 1:1–47.

Gardette J, Cousin E, Bourgin J, Torlay L, Pichat C, Moreaud O, Hot P. 2022. Hippocampal activity during memory and visual perception: the role of representational content. Cortex. 7.

Gavornik JP, Bear MF. 2014. Learned spatiotemporal sequence recognition and prediction in primary visual cortex. Nat Neurosci. 17:732–737.

Graham KS, Barense MD, Lee ACH. 2010. Going beyond LTM in the MTL: A synthesis of neuropsychological and neuroimaging findings on the role of the medial temporal lobe in memory and perception. Neuropsychologia. 48:831–853.

Grill-Spector K, Kushnir T, Hendler T, Edelman S, Itzchak Y, Malach R. 1998. A sequence of object-processing stages revealed by fMRI in the human occipital lobe. Hum Brain Mapp. 6:316–328.

Harrison SA, Tong F. 2009. Decoding reveals the contents of visual working memory in early visual areas. Nature. 458:632.

Hebscher M, Voss JL. 2020. Testing network properties of episodic memory using non-invasive brain stimulation. Curr Opin Behav Sci. 32:35–42.

Henriksson L, Nurminen L, Hyvärinen A, Vanni S. 2008. Spatial frequency tuning in human retinotopic visual areas. J Vis. 8:1–13.

Hubel DH, Wiesel TN. 1965. Receptive Architecture in Two Nonstriate Visual Areas (18 and 19) of the Cat. J Neurophysiol. 28:229–289.

Jeffreys H. 1961. Theory of Probability. 3rd ed. Oxford: Oxford University Press.

Jerde TA, Merriam EP, Riggall AC, Hedges JH, Curtis CE. 2012. Prioritized Maps of Space in Human Frontoparietal Cortex. J Neurosci. 32:17382.

Johnson JD, Rugg MD. 2007. Recollection and the reinstatement of encoding-related cortical activity. Cereb Cortex. 17:2507–2515.

Kamitani Y, Tong F. 2005. Decoding the visual and subjective contents of the human brain. Nat Neurosci. 8:679–685.

Kanwisher N. 2006. What's in a Face? Science (80-). 311:617–618.

Kanwisher N, McDermott J, Chun MM. 1997. The fusiform face area: A module in human extrastriate cortex specialized for face perception. J Neurosci. 17:4302–4311.

Karanian JM, Slotnick SD. 2018. Confident false memories for spatial location are mediated by V1. Cogn Neurosci. 9:139–150.

Kobatake E, Tanaka K. 1994. Neuronal selectivities to complex object features in the ventral visual pathway of the macaque cerebral cortex. J Neurophysiol. 71:856–867.

Kriegeskorte N, Mur M, Ruff DA, Kiani R, Bodurka J, Esteky H, Tanaka K, Bandettini PA. 2008. Matching Categorical Object Representations in Inferior Temporal Cortex of Man and Monkey. Neuron. 60:1126–1141.

Lakens D. 2013. Calculating and reporting effect sizes to facilitate cumulative science: A practical primer for t-tests and ANOVAs. Front Psychol. 4.

Le Bihan D, Turner R, Zeffiro TA, Cuenod CA, Jezzard P, Bonnerot V. 1993. Activation of human primary visual cortex during visual recall: a magnetic resonance imaging study.

Proc Natl Acad Sci U S A. 90:11802.

Lee ACH, Buckley MJ, Gaffan D, Emery T, Hodges JR, Graham KS. 2006. Differentiating the Roles of the Hippocampus and Perirhinal Cortex in Processes beyond Long-Term Declarative Memory: A Double Dissociation in Dementia. J Neurosci. 26:5198–5203.

Lee ACH, Buckley MJ, Pegman SJ, Spiers H, Scahill VL, Gaffan D, Bussey TJ, Davies RR, Kapur N, Hodges JR, Graham KS. 2005. Specialization in the medial temporal lobe for processing of objects and scenes. Hippocampus. 15:782–797.

Lee ACH, Levi N, Davies RR, Hodges JR, Graham KS. 2007. Differing profiles of face and scene discrimination deficits in semantic dementia and Alzheimer's disease. Neuropsychologia. 45:2135–2146.

Lee ACH, Scahill VL, Graham KS. 2008. Activating the medial temporal lobe during oddity judgment for faces and scenes. Cereb Cortex. 18:683–696.

Lee ACH, Yeung L-K, Barense MD. 2012. The hippocampus and visual perception. Front Hum Neurosci. 6:91.

López-Aranda MF, López-Téllez JF, Navarro-Lobato I, Masmudi-Martín M, Gutiérrez A, Khan ZU. 2009. Role of Layer 6 of V2 Visual Cortex in Object-Recognition Memory. Science (80-). 325:87–89.

Malach R, Reppas J, Benson R, Kwong K, Jiang H, Kennedy W, Ledden P, Brady T, Rosen B, Tootell R. 1995. Object-related activity revealed by functional magnetic resonance imaging in human occipital cortex. Proc Natl Acad Sci U S A. 92:8135–8139.

Mazer JA, Vinje WE, McDermott J, Schiller PH, Gallant JL. 2002. Spatial frequency and orientation tuning dynamics in area V1. Proc Natl Acad Sci. 99:1645–1650.

Morey RD, Rouder JN, Jamil X. 2015. BayesFactor: Computation of Bayes factors for

common designs.

Nadel L. 1992. Multiple Memory Systems: What and Why. J Cogn Neurosci. 4:179–188.

Nadel L, Peterson MA. 2013. The hippocampus: Part of an interactive posterior representational system spanning perceptual and memorial systems. J Exp Psychol Gen. 142:1242–1254.

Ostwald D, Lam JM, Li S, Kourtzi Z. 2008. Neural Coding of Global Form in the Human Visual Cortex. J Neurophysiol. 99:2456–2469.

Palombo DJ, Keane MM, Verfaellie M. 2015. The medial temporal lobes are critical for reward-based decision making under conditions that promote episodic future thinking. Hippocampus. 25:345–353.

Raftery AE. 1995. Bayesian Model Selection in Social Research, Source: Sociological Methodology.

Ranganath C, Ritchey M. 2012. Two cortical systems for memory-guided behaviour. Nat Rev Neurosci. 13:713–726.

Riggall AC, Postle BR. 2012. The relationship between working memory storage and elevated activity as measured with functional magnetic resonance imaging. J Neurosci. 32:12990–12998.

Ritchey M, Montchal ME, Yonelinas AP, Ranganath C. 2015. Delay-dependent contributions of medial temporal lobe regions to episodic memory retrieval. Elife. 4:1–19.

Rosenthal R. 1994. Parametric measures of effect size. In: Cooper H,, Hedges L V.,, Valentine JC, editors. The handbook of research synthesis. New York: Russell Sage Foundation. p. 231–244.

Ross DA, Sadil P, Wilson DM, Cowell RA. 2018. Hippocampal engagement during recall

depends on memory content. Cereb Cortex. 28:2685–2698.

Rugg MD, Vilberg KL. 2013. Brain networks underlying episodic memory retrieval. Curr Opin Neurobiol. 23:255–260.

Schapiro AC, Gregory E, Landau B, McCloskey M, Turk-Browne NB. 2014. The Necessity of the Medial Temporal Lobe for Statistical Learning. J Cogn Neurosci. 26:1736–1747.

Serences JT, Ester EF, Vogel EK, Awh E. 2009. Stimulus-Specific Delay Activity in Human Primary Visual Cortex. Psychol Sci. 20:207.

Serences JT, Saproo S, Scolari M, Ho T, Muftuler LT. 2009. Estimating the influence of attention on population codes in human visual cortex using voxel-based tuning functions. Neuroimage. 44:223–231.

Sherry DF, Schacter DL. 1987. The Evolution of Multiple Memory Systems. Psychol Rev. 94:439–454.

Shimamura AP. 2011. Episodic retrieval and the cortical binding of relational activity. Cogn Affect Behav Neurosci. 11:277–291.

Sprague TC, Ester EF, Serences JT. 2014. Reconstructions of information in visual spatial working memory degrade with memory load. Curr Biol. 24:2174–2180.

Squire LR, Zola-Morgan S. 1991. The medial temporal lobe memory system. Science (80-). 253:1380–1386.

Staresina BP, Cooper E, Henson RN. 2013. Reversible Information Flow across the Medial Temporal Lobe: The Hippocampus Links Cortical Modules during Memory Retrieval. J Neurosci. 33:14184–14192.

Staresina BP, Duncan KD, Davachi L. 2011. Perirhinal and Parahippocampal Cortices Differentially Contribute to Later Recollection of Object- and Scene-Related Event

Details. J Neurosci. 31:8739–8747.

Stark CE, Squire LR. 2001. When zero is not zero: the problem of ambiguous baseline conditions in fMRI. Proc Natl Acad Sci U S A. 98:12760–12766.

Thakral PP, Madore KP, Addis DR, Schacter DL. 2020. Reinstatement of Event Details during Episodic Simulation in the Hippocampus. Cereb Cortex. 30:2321–2337.

Thakral PP, Slotnick SD, Schacter DL. 2013. Conscious processing during retrieval can occur in early andlate visual regions. Neuropsychologia. 51:482–487.

Thakral PP, Wang TH, Rugg MD. 2017. Decoding the content of recollection within the core recollection network and beyond. Cortex. 91:101–113.

Tulving E. 1987. Multiple memory systems and consciousness. Hum Neurobiol.

Tulving E, Schacter DL. 1990. Priming and human memory systems. Science (80-). 247:301–306.

Wagenmakers EJ, Marsman M, Jamil T, Ly A, Verhagen J, Love J, Selker R, Gronau QF, Šmíra M, Epskamp S, Matzke D, Rouder JN, Morey RD. 2017. Bayesian inference for psychology. Part I: Theoretical advantages and practical ramifications. Psychon Bull Rev 2017 251. 25:35–57.

Wang L, Mruczek REB, Arcaro MJ, Kastner S. 2015. Probabilistic maps of visual topography in human cortex. Cereb Cortex. 25:3911–3931.

Williams P. 1998. Representational organization of multiple examplars of object categories. 1–21.